Strain compensated robust semiconductor saturable absorber mirror for fiber lasers

Yan Wang (王 燕)[1], Nan Lin (林 楠)[2], Wanli Gao (高婉丽)[1], Huanyu Song (宋寰宇)[3], Minglie Hu (胡明列)[3], Haiming Li (黎海明)[4], Wenxia Bao (包文霞)[4], Xiaoyu Ma (马骁宇)[2], and Zhigang Zhang (张志刚)[1,*]

[1]*State Key Laboratory of Advanced Optical Communication Systems and Networks, School of Electronics Engineering and Computer Science, Peking University, Beijing 100871, China*

[2]*National Research Center for Optoelectronic Engineering, Institute of Semiconductors, Chinese Academy of Sciences, Beijing 100871, China*

[3]*Ultrafast Laser Laboratory, Key Laboratory of Opto-electronic Information Technical Science of Ministry of Education, School of Precision Instrument and Opto-electronics Engineering, Tianjin University, Tianjin 300072, China*

[4]*Huakuai Photonic Technologies Inc., Zhongshan 528400, China*

**Corresponding author: zhgzhang@pku.edu.cn*

Received March 6, 2019; accepted March 28, 2019; posted online June 25, 2019

We demonstrate a strain compensated long lifetime semiconductor saturable absorber mirror (SESAM) with a high modulation depth for fiber lasers. The SESAM was measured to have a damage threshold of 9.5 mJ/cm^2, a modulation depth of 11.5%, a saturation fluence of 39.3 μJ/cm^2, and an inversed saturable absorption coefficient of 630 mJ/cm^2. The SESAM has been applied to a linear cavity mode-locked Yb-doped fiber laser, which has been working for more than a year without damage of the SESAM.

OCIS codes: 140.4050, 140.3510, 160.6000.
doi: 10.3788/COL201917.071404.

Femtosecond and picosecond mode-locked lasers have been widely used in scientific and industrial areas[1–5]. The demand for highly reliable and long lifetime mode-locked lasers is increasing. Semiconductor saturable absorber mirror (SESAM) plays a key role in passively mode-locked lasers[6–9]. Since 1992, extensive theoretical and experimental studies have been conducted on SESAM mode-locked fiber lasers[10–14]. However, the operation of SESAM mode-locked lasers can be interrupted due to the damage of the SESAM. Not only do the high power laser oscillators face this problem, the low power mode-locked laser oscillators also face the same challenge. Although the intra-cavity power density is much lower than the damage threshold of the SESAM in those lasers, the giant pulses emerging in the *Q*-switch process before the mode locking can bring high power density, which causes damage to the SESAM. To this end, a high damage threshold SESAM is required to guarantee a long lifetime of the laser oscillators. High damage threshold SESAMs for solid state lasers have been developed and tested in mode-locked Yb-doped thin-disk lasers[15–17]. So far, the high damage threshold SESAM for fiber lasers has not been reported yet.

SESAMs for mode-locked fiber lasers require much higher modulation depth, which means thicker absorption layers or large number of quantum wells (QWs). However, due to the lattice mismatch between the QWs and the substrate, more strain will be accumulated in both the thick layer and multiple QWs in this situation. Such strain can bring defects, misfit locations, as well as poor surface morphology in the epitaxial layers, and also has been one of the main limitations for a higher damage threshold[18,19]. The strain compensated InGaAs/GaAsP multi-QWs can reduce the energy of accumulative strain, making the threading-dislocation-free high strain multi-QWs possible[20,21]. Besides, the two-photon absorption in the transparent layers is also one of the most important factors causing damage on the SESAM. To solve this problem, we replaced the transparent space layer with a lower nonlinearity one. The materials with lower refractive index have a lower nonlinearity. Therefore, AlGaAsP, which has a lower refractive index than the commonly used GaAsP, is preferred. Based on the aforementioned consideration, although both AlGaAsP and GaAsP can be used as strain compensation layers, AlGaAsP is better for its lower refractive index.

In this work, we propose a SESAM structure with strain compensated InGaAs/GaAsP multi-QWs. The SESAM was characterized using femtosecond laser pulses with a modulation depth of 11.5% and a damage threshold of 9.5 mJ/cm^2. The SESAM has been tested in a picosecond mode-locked fiber laser, which has been working for a year or so without seeing damage on the SESAM, proving the long lifetime of the SESAM.

The structure of the SESAM is shown in Fig. 1. The bottom mirror is a distributed Bragg reflector (DBR), consisting of 27 pairs of GaAs/AlGaAs. The absorber segment has eight cycles of half-wave thickness. Each cycle contains two QWs spaced by thin GaAsP layers. There is AlGaAsP at both sides of each cycle as the strain

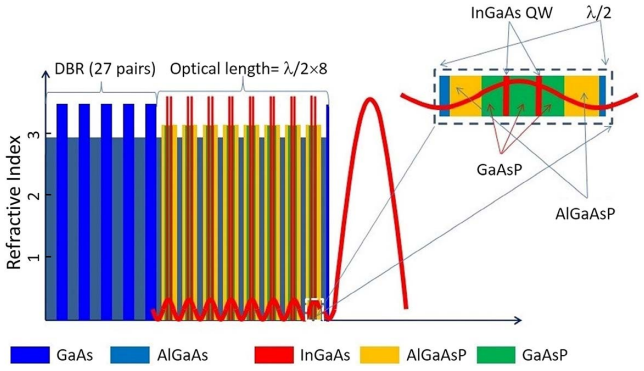

Fig. 1. Designed structure of the SESAM.

compensation layers. All QWs are arranged in the peak of the standing wave in the layers. Between the strain compensation layers, there are also AlGaAs space layers.

The SESAM was grown on GaAs (100) substrates by means of metal–organic chemical vapor deposition (MOCVD). The growth temperature was 690°C for GaAs/AlGaAs DBRs, buffers, and caps and 580°C for InGaAs/GaAsP QWs.

The key parameters of the SESAM are the saturation fluence F_{sat}, the saturated reflectivity R_{ns}, the linear reflectivity R_{lin}, the modulation depth β ($\beta = R_{\mathrm{ns}} - R_{\mathrm{lin}}$), the non-saturable loss $1 - R_{\mathrm{ns}}$, the damage threshold F_d, and the inversed saturable absorption (ISA) coefficient F_2[16]. As to the SESAM for mode-locked fiber lasers, a large modulation depth β, a proper saturation fluence F_{sat}, and a lower non-saturable loss R_{ns} are required. Besides, a higher ISA coefficient F_2, which results in a high damage threshold F_d, is also significant for improving the lifetime of the SESAM.

Based on Eq. (1), the parameters can be derived from the measurement of the reflectivity as a function of the incident fluence, but numerical correction for a Gaussian-shaped beam is needed[22]:

$$R(F) = R_{\mathrm{ns}} \frac{\ln[1 + R_{\mathrm{lin}}/R_{\mathrm{ns}}(e^{F/F_{\mathrm{sat}}} - 1)]}{F/F_{\mathrm{sat}}} e^{-F/F_2}. \quad (1)$$

Following the method in Ref. [23], we built up a characterization setup, which is shown in Fig. 2. The system consists of a mode-locked fiber laser, two variable attenuation stages, and two photodetectors. The mode-locked Yb-doped fiber laser has a center wavelength of 1064 nm and 2.5 W average power at 500 kHz repetition rate, corresponding to a pulse energy of 5 μJ. The pulse duration is 300 fs.

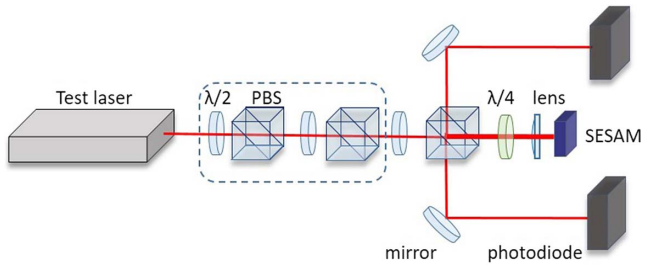

Fig. 2. Experimental setup for characterization of the SESAM. Test laser, 1064 nm mode-locked fiber laser with a pulse energy of 5 μJ; $\lambda/2$, half-wave plate; $\lambda/4$, quarter-wave plate; PBS, polarization beam splitter; lens, with a 30 mm focal length.

We can adjust the pulse fluence to more than four magnitudes through altering the two attenuation stages. The laser beam was divided into a reference arm and a signal arm using a half-wave plate and a polarization beam splitter. A lens of 30 mm focal length was used to focus the beam onto the SESAM with a spot diameter of 34 μm, which allowed the pulse fluence up to hundreds of millijoules per centimeter squared (mJ/cm^2). A silver mirror with the reflectivity of 95% was used to calibrate the detection system. The measured nonlinear reflectivity is shown in Fig. 3. The derived parameters for the SESAM are shown in Table 1.

We constructed a linear cavity mode-locked Yb-doped fiber laser to test the SESAM. The structure of the laser is shown in Fig. 4. The SESAM was mounted on a copper heat sink. A lens with a focal length of 15 mm focused the beam onto the SESAM with a spot size of 20 μm, achieving a pulse fluence of 300 μJ/cm^2. The collimator, the lens, and the SESAM were integrated into a small module with a fiber pigtail (Fig. 5). The other end of the cavity was a fiber grating centered at 1064 nm, and the reflection bandwidth was 0.4 nm. The total reflectivity was 90%, which allows for 10% of the output coupling. The Yb-doped fiber was a 70 cm long single mode

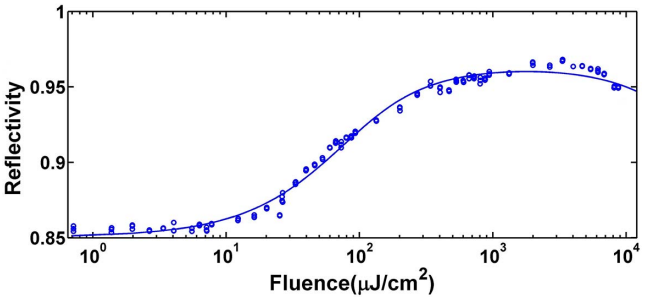

Fig. 3. Nonlinear reflectivity measurements for the SESAM under test. The reflectivity is fitted with Eq. (1).

Table 1. Derived SESAM Parameters

Parameters	Measured Results
Saturation fluence F_{sat}	39.3 μJ/cm^2
Saturated reflectivity R_{ns}	96.5%
Linear reflectivity R_{lin}	85.0%
Modulation depth β	11.5%
Non-saturable loss $1 - R_{\mathrm{ns}}$	3.5%
Damage threshold F_d	9.5 mJ/cm^2
ISA coefficient F_2	6.3×10^2 mJ/cm^2

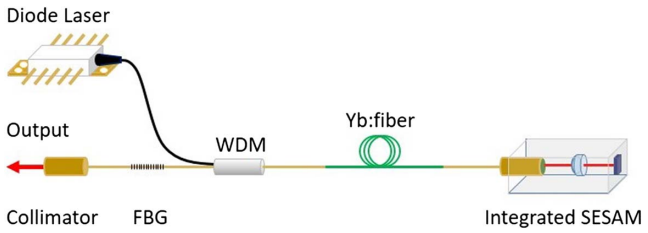

Fig. 4. Experimental setup of the mode-locked laser based on SESAM. Integrated SESAM including a 1064 nm collimator, a lens with a 15 mm focal length, and a SESAM mounted on a copper heat sink; Yb:fiber, Yb-doped fiber with an absorption coefficient of 5 dB/m at 975 nm; WDM, wavelength division multiplexer; FBG, fiber grating with a center wavelength of 1064 nm; diode laser, with a center wavelength at 975 nm.

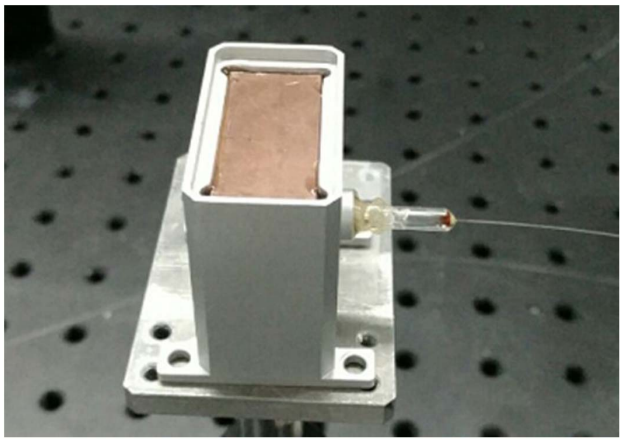

Fig. 5. Image of the integrated SESAM.

polarization maintaining fiber with an absorption coefficient of 5 dB/m at 975 nm. The total fiber length was 260 cm, making the pulse repetition rate of 38 MHz.

The laser starts mode locking at a pump power of 120 mW, and the mode locking is very stable (Fig. 6). Figure 7(a) is the measured spectrum of the pulse. The pulse width is measured as 19.92 ps by an autocorrelation with an assumed Gaussian pulse profile [Fig. 7(b)]. Figure 7(c) is the measurement of output power as a function of pump power.

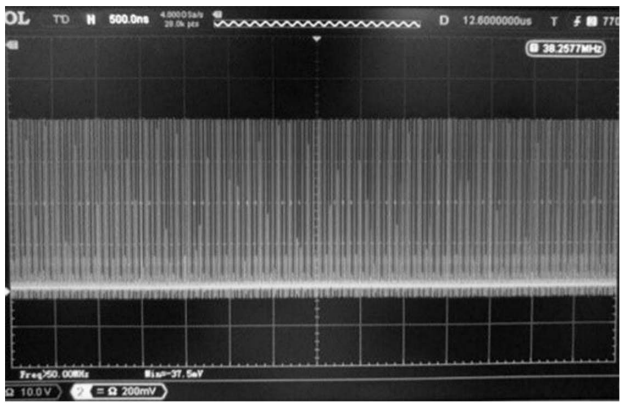

Fig. 6. Pulse sequences from the SESAM mode-locked laser.

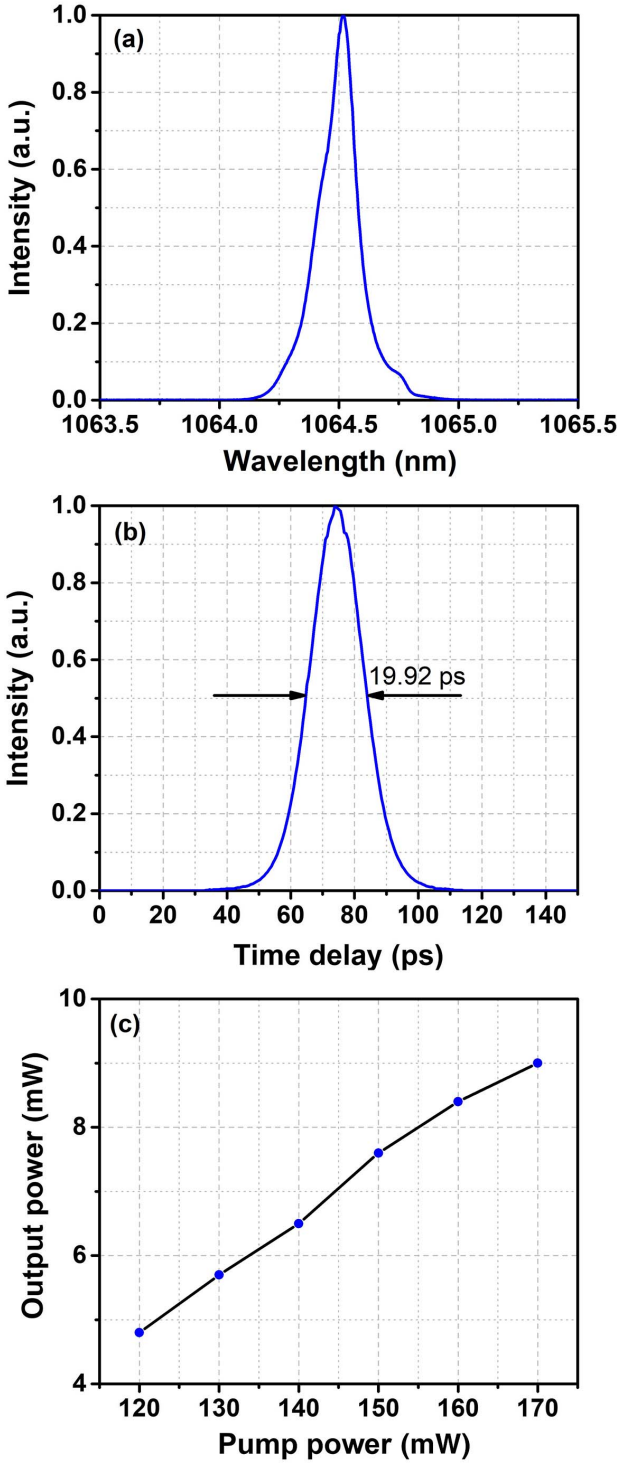

Fig. 7. (a) Measured pulse spectrum of the pulse train from the laser oscillator. (b) Intensity autocorrelation trace of the pulse train. (c) Measurement of output power as a function of pump power.

The output power at 170 mW pump power is 9 mW, and further higher pump power makes the laser unstable. The laser has been running for more than a year, which proves the long lifetime of the SESAM.

In summary, we demonstrated a SESAM by the design of strain compensated InGaAs/GaAsP multi-QWs.

The SESAM has a high damage threshold up to 9.5 mJ/cm^2, a modulation depth of 11.5%, a saturation fluence of 39.3 μJ/cm^2, and an ISA coefficient of 630 mJ/cm^2. The SESAM has been installed into a linear cavity Yb-doped mode-locked fiber laser and has been operated for more than a year. The laser experiment proves the long lifetime of the SESAM and allows the laser to be an excellent seed for further amplification.

This work was supported by the National Natural Science Foundation of China (Nos. 61575004, 61735001, and 61761136002) and the International Cooperation Program (No. 2013DFG12750).

References

1. K. C. Phillips, H. H. Gandhi, E. Mazur, and S. K. Sundaram, Adv. Opt. Photon. **7**, 684 (2015).
2. F. Helmchen and W. Denk, Nat. Methods **2**, 932 (2005).
3. K. Minoshima and H. Matsumoto, Appl. Opt. **39**, 5512 (2000).
4. J. Kim, J. A. Cox, J. Chen, and F. X. Kärtner, Nat. Photon. **2**, 733 (2008).
5. T. Südmeyer, S. V. Marchese, S. Hashimoto, C. R. E. Baer, G. Gingras, B. Witzel, and U. Keller, Nat. Photon. **2**, 599 (2008).
6. Y. Bai, W. Xiang, P. Zu, and G. Zhang, Chin. Opt. Lett. **10**, 111405 (2012).
7. Y. Xue, Q. Wang, Z. Zhang, L. Chai, Z. Wang, Y. Han, H. Sun, J. Li, J. Wang, Y. Wang, X. Ma, and Y. Song, Chin. Opt. Lett. **2**, 466 (2004).
8. G. Ju, L. Chai, Q. Wang, Z. Zhang, Y. Wang, and X. Ma, Chin. Opt. Lett. **1**, 695 (2003).
9. U. Keller, Nature **424**, 831 (2003).
10. U. Keller, D. A. B. Miller, G. D. Boyd, T. H. Chiu, J. F. Ferguson, and M. T. Asom, Opt. Lett. **17**, 505 (1992).
11. K. J. Weingarten, U. Keller, T. H. Chiu, and J. F. Ferguson, Opt. Lett. **18**, 640 (1993).
12. U. Keller, K. J. Weingarten, F. X. Kärtner, D. Kopf, B. Braun, I. D. Jung, R. Fluck, C. Hönninger, N. Matuschek, and J. Aus der Au, IEEE J. Sel. Top. Quantum Electron. **2**, 435 (1996).
13. V. Pusino, M. J. Strain, and M. Sorel, Photon. Res. **2**, 186 (2014).
14. L. Chen, M. Zhang, X. Wang, W. Li, Y. Wei, Y. Ma, Z. Fan, G. Niu, J. Yu, Y. Liu, Z. Xue, and Z. Zhang, Chin. Sci. Bull. **561**, 348 (2011).
15. C. J. Saraceno, C. Schriber, M. Mangold, M. Hoffmann, O. H. Heckl, C. R. E. Baer, M. Golling, T. Südmeyer, and U. Keller, IEEE J. Sel. Top. Quantum Electron. **18**, 29 (2012).
16. C. G. E. Alfieri, A. Diebold, F. Emaury, E. Gini, C. J. Saraceno, and U. Keller, Opt. Express **24**, 27587 (2016).
17. C. J. Saraceno, F. Emaury, C. Schriber, M. Hoffmann, M. Golling, T. Südmeyer, and U. Keller, Opt. Lett. **39**, 9 (2014).
18. C. G. E. Alfieri, A. Diebold, M. Kopp, D. Waldburger, M. Mangold, F. Emaury, C. J. Saraceno, E. Gini, and U. Keller, in *Conference on Lasers and Electro-Optics* (2016), p. 1.
19. T. Diebold, M. Zengerle, M. Mangold, C. Schriber, F. Emaury, M. Hoffmann, C. J. Saraceno, M. Golling, D. Follman, G. D. Cole, M. Aspelmeyer, T. Südmeyer, and U. Keller, Opt. Express **24**, 10512 (2016).
20. H. Asano, M. Wada, T. Fukunaga, and T. Hayakawa, Appl. Phys. Lett. **74**, 3090 (1999).
21. H. C. Kuo, Y. H. Chang, H. H. Yao, Y. A. Chang, F. I. Lai, M. Y. Tsai, and S. C. Wang, IEEE Photon. Tech. Lett. **17**, 528 (2005).
22. M. Haiml, R. Grange, and U. Keller, Appl. Phys. B **79**, 331 (2004).
23. D. J. H. C. Maas, B. Rudin, A.-R. Bellancourt, D. Iwaniuk, S. V. Marchese, T. Südmeyer, and U. Keller, Opt. Express **16**, 7571 (2008).